*IOSR Journal of Electrical and Electronics Engineering (IOSR-JEEE)*
*e-ISSN: 2278-1676,p-ISSN: 2320-3331, Volume 7, Issue 6 (Sep. - Oct. 2013), PP 91-97*
*www.iosrjournals.org*

# Design and MATLAB Simulation of a Fuel Cell Based Interleaved Buck Converter with Low Switching Losses and Improved Conversion Ratio

Jinimol Jose[1], Dr. Mini K Idikkula[2]
[1]*( Electrical and Electronics Engineering,Govt.Engineering College Idukki/M.G.University, India)*
[2]*(Electrical and Electronics Engineering, Govt.Engineering College Idukki / M.G.University, India)*

***Abstract:*** *The Interleaved Buck Converter (IBC) having low switching losses and improved step-down conversion ratio is suitable for the applications where the input voltage is high and the operating duty is below 50%. It is similar to the conventional IBC, but two active switches are connected in series and a coupling capacitor is employed in the power path. This IBC shows that since the voltage stress across all the active switches is half of the input voltage before turn-on or after turn-off when the operating duty is below 50%, the capacitive discharging and switching losses can be reduced considerably. This allows the IBC to have higher efficiency and operate with higher switching frequency. In addition, it has a higher step-down conversion ratio and a smaller output current ripple compared with a conventional IBC. Closed loop control using PI controller has been done to improve the system performances. By replacing the conventional voltage source by a renewable one will enhance its reliability and is more economical. So here the dynamics of a polymer electrolyte membrane fuel cell (PEM Fuel cell) is modelled, simulated and presented. MATLAB –SIMULINK is used for the modelling and simulation of the fuel cell stack. Design and analysis of the converter is done for a DC input of 200V and duty ratio D<0.5. The expected output DC voltage is 24V/10A. Simulation of both conventional and new IBC is done using MATLAB/SIMULINK and their outputs are compared.*

***Keywords :*** *Buck converter, Fuel cell stack, Interleaved, Low switching loss.*

## I. INTRODUCTION

Interleaved buck converter (IBC) has received a lot of attention in applications where non-isolation, step-down conversion ratio, and high output current with low ripple are required, due to its simple structure and low control complexity. However, in the conventional IBC, all semiconductor devices suffer from the input voltage, and hence, high-voltage devices rated above the input voltage should be used. High-voltage-rated devices have generally poor characteristics such as high cost, high on-resistance, high forward voltage drop, severe reverse recovery, etc. In addition, the converter operates under hard switching condition. Thus, the cost becomes high and the efficiency becomes poor. And, for higher power density and better dynamics, it is required that the converter operates at higher switching frequencies. However, higher switching frequencies increase the switching losses associated with turn-on, turn-off, and reverse recovery. Consequently, the efficiency is further deteriorated. Also, it experiences an Extremely short duty cycle in the case of high input and low-output voltage applications.

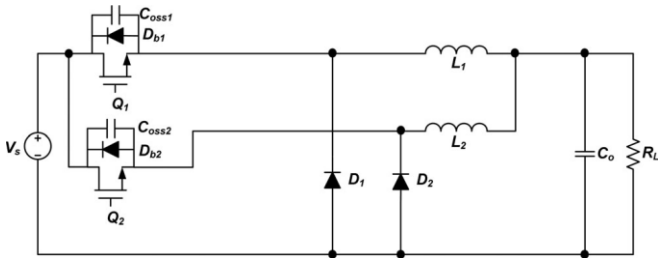


Fig. 1. Conventional IBC

To overcome the aforementioned drawbacks of the conventional IBC, some pieces of research for reducing the voltage stress of a buck converter and several kinds of IBCs have been presented until now. In three-level buck converters the voltage stress is half of the input voltage. However, so many components are required for the use of IBC. An IBC with a single-capacitor turnoff snubber is introduced. Its advantages are that the switching loss associated with turn-off transition can be reduced, and single coupled inductor implements the converter as two output inductors. However, since it operates at discontinuous conduction mode (DCM), all elements suffer from high-current stress, resulting in high conduction and core losses. In addition, the voltages

across all semiconductor devices are still the input voltage. Then an IBC with active-clamp circuits is introduced. In the converter, all active switches are turned ON with zero-voltage switching (ZVS). In addition, a high step-down conversion ratio can be obtained and the voltage stress across the freewheeling diodes can be reduced. However, in order to obtain the mentioned advantages, it requires additional passive elements and active switches, which increases the cost significantly at low or middle levels of power applications. IBC with zero-current transition (ZCT) is introduced to reduce diode reverse recovery losses. The ZCT is implemented by only adding an inductor into the conventional IBC. However, in spite of these advantages, the converter suffers from high current stress, because the output current flows through each module in a complementary way. And it still has the drawbacks of the conventional IBC. An IBC with two winding coupled inductors is introduced. The converter has the following advantages. Since it operates at continuous conduction mode (CCM), the current stress is lower than that of DCM IBC. The voltages across all semiconductor devices can be reduced by adjusting the turn ratio of the coupled inductors, which allows that although it operates with hard switching, the switching losses can be reduced. Additionally, a high step-down conversion ratio can also be obtained.

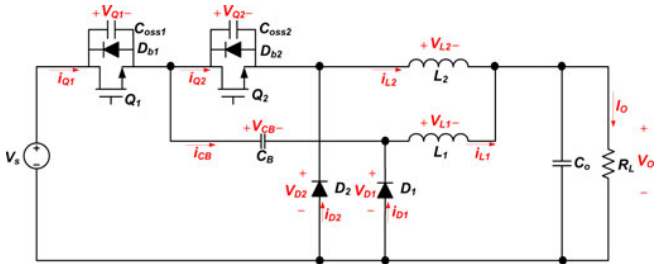


Fig. 2. Proposed IBC

So a new IBC, which is suitable for the applications where the input voltage is high and the operating duty is below 50%, is proposed. It is similar to the conventional IBC, The two active switches are driven with the phase shift angle of 180◦ and the output voltage is regulated by adjusting the duty cycle at a fixed switching frequency. Since the proposed IBC also operates at CCM, the current stress is low. During the steady state, the voltage stress across all active switches before turn-on or after turn-off is half of the input voltage. Thus, the capacitive discharging and switching losses can be reduced considerably. The voltage stress of the freewheeling diodes is also lower than that of the conventional IBC but two active switches are connected in series and a coupling capacitor is employed in the power path.so that the reverse-recovery and conduction losses on the freewheeling diodes can be improved by employing schottky diodes that have generally low breakdown voltages, typically below 200V. The conversion ratio and output current ripple are lower than those of the conventional IBC.

Also, rapid growth in energy consumption during the last century on the one hand, and limited resources of energy on the other, has caused many concerns and issues today. Although the conventional sources of energy, such as fossil fuels, are currently available in vast quantities, however they are not unlimited and sooner or later will vanish. Renewable energy sources are the answer to these needs and concerns, since they are available as long as the sun is burning, and because they are sustainable as they have no or little impact on the environment. One technology which can be based upon sustainable sources of energy is fuel cell.

One technology which can be based upon sustainable sources of energy is fuel cell. Fuel cells are devices that directly convert the chemical energy stored in some fuels into electrical energy and heat. The preferred fuel for many fuel cells is hydrogen, and hydrogen fuel is a renewable source of energy; hence fuel cell technology has received a considerable attention in recent years. PEM fuel cell is considered to be a promising power source, especially for transportation and stationary cogeneration applications due to its high efficiency, low temperature operation, high power density, fast startup, and system robustness.

By examining all the advantages of the fuel cell based system, we thought of working on it as we believe that in near future, the scarcity of power will force the whole world to move to other alternatives for power.

## II. CIRCUIT OPERATIONS

Fig. 2 shows the circuit configuration of the proposed IBC. The structure is similar to a conventional IBC except two active switches in series and a coupling capacitor employed in the power path. Switches $Q1$ and $Q_2$ are driven with the phase shift angle of 180◦. This is the same as that for a conventional IBC. Each switching period is divided into four modes, whose operating circuits are shown in Fig. 4. In order to illustrate the operation of the proposed IBC, some assumptions are made as follows:

1) the output capacitor $C_O$ is large enough to be considered as a voltage source;
2) the two inductors $L_1$ and $L_2$ have the same inductance $L$;

3) all power semiconductors are ideal;
4) the coupling capacitor $C_B$ is large enough to be considered as a voltage source.

**1.1. Steady-State Operation when D≤0.5**

Mode 1 [$t_0$ –$t_1$ ]: Mode 1 begins when $Q_1$ is turned ON at $t_0$ . Then, the current of $L_1$ , $i_{L1}$ (t), flows through$Q_1$ , $C_B$ , and $L_1$ and the voltage of the coupling capacitor $V_{CB}$ is charged. The current of $L_2$ , $i_{L2}$ (t), freewheels through $D_2$ . During this mode, the voltage across $L_1$ , $V_{L1}$ (t), is the difference of the input voltage $V_S$ , the voltage of the coupling capacitor $V_{CB}$, and the output voltage VO , and its level is positive. Hence, $i_{L1}$ (t) increases linearly from the initial value. The voltage across $L_2$ , $V_{L2}$ (t), is the negative output voltage, and hence, $i_{L2}$ (t) decreases linearly from the initial value. The voltage across $Q_2$ , $V_{Q2}$ (t), becomes the input voltage and the voltage across $D_1$ , $V_{D1}$ (t), is equal to the difference of $V_S$ and $V_{CB}$. The voltages and currents can be expressed as follows:

$$V_{L1}(t) = V_S - V_{CB} - V_O \quad (1)$$

$$V_{L2}(t) = -V_O \quad (2)$$

$$V_{Q2} = V_S \quad (3)$$

$$V_{D1} = V_S - V_{CB} \quad (4)$$

*Mode 2 [$t_1$ –$t_2$ ]*: Mode 2 begins when $Q_1$ is turned OFF at $t_1$ . Then, $i_{L1}$ ($t$) and $i_{L2}$ ($t$) freewheel through $D_1$ and $D_2$, respectively. Both $V_{L1}$ ($t$) and $V_{L2}$ ($t$) become the negative $V_O$ , and hence, $i_{L1}$ ($t$) and $i_{L2}$ ($t$) decrease linearly. During this mode, the voltage across $Q_1$ , $V_{Q1}$ ($t$), is equal to the difference of $V_S$ and $V_{CB}$ and $V_{Q2}$ ($t$) becomes $V_{CB}$. The voltages and currents can be expressed as follows:

$$V_{L1}(t) = V_{L2}(t) = -V_O \quad (5)$$

$$V_{Q1}(t) = V_S - V_{CB} \quad (6)$$

$$V_{Q2}(t) = V_{CB} \quad (7)$$

*Mode 3 [$t_2$ –$t_3$ ]:* Mode 3 begins when $Q_2$ is turned ON at $t_2$ . At the same time, $D_2$ is turned OFF. Then, $i_{L1}$ ($t$) freewheels through $D_1$ and $i_{L2}$ ($t$) flows through $D_1$ , $C_B$ , $Q_2$ , and $L_2$.Thus, $V_{CB}$ is discharged. During this mode, $V_{L2}$ ($t$) is equal to the difference of $V_{CB}$ and $V_O$ and its level is positive. Hence, $i_{L2}$ ($t$) increases linearly. $V_{L1}$ ($t$) is the negative $V_O$,and hence, $i_{L1}$ (t) decreases linearly. The voltages and currents can be expressed as follows:

$$V_{L1}(t) = -V_O \quad (8)$$

$$V_{L2}(t) = V_{CB} - V_O \quad (9)$$

$$V_{Q1} = V_S - V_{CB} \quad (10)$$

$$V_{Q2} = V_{CB} \quad (11)$$

Mode 4 [$t_3$ –$t_4$ ]: Mode 4 begins when $Q_2$ is turned OFF at $t_3$ , and its operation is the same with that of mode 2.

The steady-state operation of the proposed IBC operating with the duty cycle of $D \leq 0.5$ has been described. From the operation principles, it is known that the voltage stress of all semiconductor devices except $Q_2$ is not the input voltage, but is determined by the voltage of coupling capacitor $V_{CB}$. The maximum voltage of $Q_2$ is the input voltage, but the voltage before turn-on or after turn-off is equal to $V_{CB}$. As these results, the capacitive discharging and switching losses on $Q_1$ and $Q_2$ can be reduced considerably. In addition, since diodes with good characteristics such as schottky can be used for $D_1$ and $D_2$ , the reverse-recovery and conduction losses can be also improved.

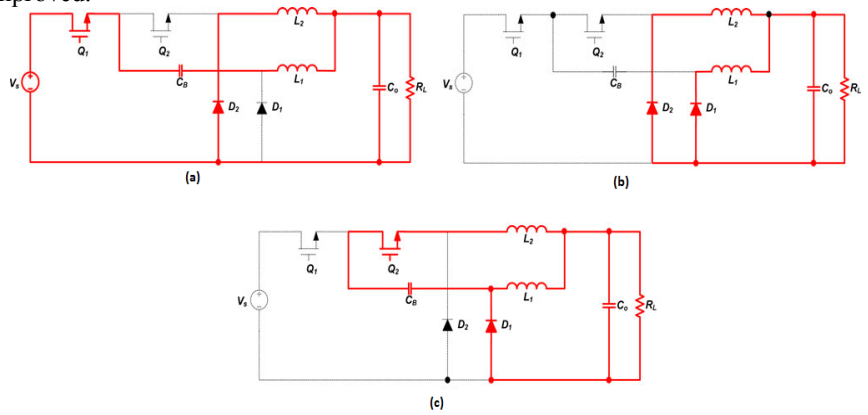


Fig.3. Operating Circuits of New IBC when $D \leq 0.5$. (a) Mode 1. (b) Mode 2 or 4. (c) Mode 3.

## III. DESIGN AND ANALYSIS

### 3.1. DC Conversion Ratio

Then, the dc conversion ratio *M* is calculated as:

$$M = \frac{V_O}{V_S} = \frac{D}{2} \quad (13)$$

In the case of conventional IBC, the dc conversion ratio M is given as follows,

$$M = \frac{V_O}{V_S} = D \quad (14)$$

From (13) and (14) it is clear that the proposed IBC has a higher step-down conversion ratio than the conventional IBC. As a result ,the the proposed IBC can overcome the extremely short duty cycle, which appears in the conventional IBC.

### 3.2. Inductor Current Ripple

Fig. 4. shows the voltage and current waveforms of the output inductor of the buck converter. From the figure, the current ripple can be expressed as follows:

$$\Delta_{iripple} = \frac{V_{k1}}{L} D_k T_S \quad (15)$$

In the case of D≤0.5, the parameters for the proposed IBC are as follows:

$$Vk_1 = 0.5V_S - V_O;\ Vk_2 = V_O;\ Dk = D. \quad (16)$$

The parameters for the conventional IBC can be expressed as

$$V_{k1} = V_S - V_O;\ V_{k2} = V_O;\ D_k = 0.5D. \quad (17)$$

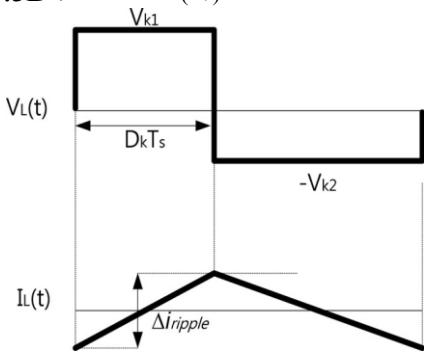


Fig.4. Voltage and current waveforms of the output inductor of the buck converter.

### 3.3. Coupling Capacitor

The ripple voltage of the coupling capacitor is calculated as follows:

$$\Delta V_{CB} = \frac{1}{C_B}\int_{t0}^{t1} i_{CB}(t)dt = \frac{I_O D}{2C_B f_s} \quad (18)$$

From (18), it is known that although a capacitor with low capacitance is used for $C_B$ , the voltage ripple can be reduced by increasing the switching frequency.

### 3.4. Stress and Loss Analysis

For stress and loss analysis, it is assumed that the IBCs operate with the duty cycle of $D \leq 0.5$.

It is investigated that due to the improved voltage waveforms in the proposed IBC, the capacitive discharging and switching losses are reduced. Also, it can be seen that at higher switching frequency, the increased losses in the proposed IBC are much smaller than those in the conventional IBC. This means that the proposed converter can operate at higher switching frequencies without the penalty of a significant increase in the losses. Thus, it can be said that the propose IBC is more advantageous in terms of efficiency and power density compared with the conventional IBC.

## IV. CLOSED LOOP CONTROL OF THE CONVERTER

### 4.1. PI Controller

PI Controller (proportional-integral controller) is a feedback controller which drives the plant to be controlled by a weighted sum of the error (difference between the output and desired set-point) and the integral of that value which is given by equation (19). It is a special case of the PID controller in which the derivative

(D) part of the error is not used. Integral control action added to the proportional controller converts the original system into high order. Hence the control system may become unstable for a large value of *KP* since roots of the characteristic eqn. may have positive real part. In this control, proportional control action tends to stabilize the system, while the integral control action tends to eliminate or reduce steady-state error in response to various inputs.

$G_{PI}(s) = Kp + Ki/s$ (19)

A proportional controller ($K_P$ ) will have the effect of reducing the rise time, but never eliminate the steady-state error. An integral control ($K_I$ ) will have the effect of eliminating the steady-state error, but it may make the transient response worse.

## V. FUEL CELL

### 5.1. Mathematical Model of A Fuel Cell

The fundamental structure of a PEM fuel cell can be described as two electrodes (anode and cathode) separated by a solid membrane acting as an electrolyte (Fig.6). Hydrogen fuel flows through a network of channels to the anode, where it dissociates into protons that, in turn, flow through the membrane to the cathode and electrons that are collected as electrical current by an external circuit linking the two electrodes. The oxidant (air in this study) flows through a similar network of channels to the cathode where oxygen combines with the electrons in the external circuit and the protons flowing through the membrane, thus producing water.

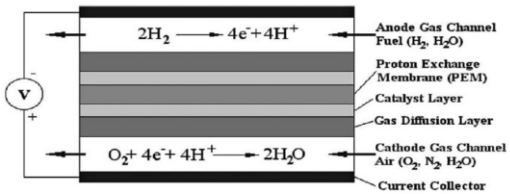


Fig.5. Schematic of a Single PEM Fuel Cell

Electrons flowing from the anode towards the cathode provide power to the load. A number of cells, when connected in series, make up a stack and deliver sufficient electricity. A I-V curve, known as a polarization curve, is generally used to express the characteristics of a fuel cell (Fig. 6). The behavior of a cell is highly non-linear and dependant on a number of factors such as current density, cell temperature, membrane humidity, and reactant partial pressure.

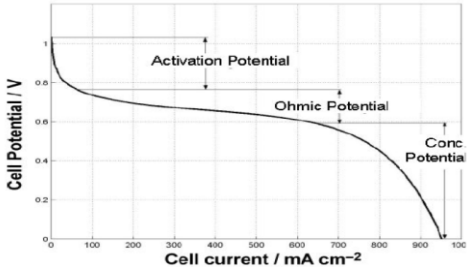


Fig. 6. Polarization Curve

The cell potential ($V_{cell}$), at any instance could be found using Eq. 22 When a cell delivers power to the load, the no-load voltage (E), is reduced by three classes of voltage drop, namely, the activation ($V_{act}$), ohmic ($V_{ohm}$), and concentration ($V_{conc}$) over voltages.

$V_{cell} = E - V_{act} - V_{ohm} - V_{conc}$ V (20)

The Nerst equation (Eq. 21) gives the open circuit cell potential (E) as a function of cell temperature (T) and the reactant partial pressures.

$$E = E_O - 0.85\square 10^{-3(T-298.15)} + (\frac{RT}{2F})\ln(Q) \quad (21)$$

Where,

$$Q = \frac{P_{H2} \cdot p_{O2}{}^{0.5}}{P_{H_2O} \cdot P^{0.5}} \quad (22)$$

Then,

$$E_{act} = 0.9514 + 0.00312T - 0.000187T[\ln(I)] + 7.4 \cdot 10^{-5} T[\ln(C_{O_2})] \quad (23)$$

And,

$V_{conc} = a \cdot e^{b1}$ V (24)

Where,

$a = 1.1 \cdot 10^{-4} - 1.2 \cdot 10^{-6}(T - 273)$ (25)

$b = 8 \cdot 10^{-3}$ (26)

If all the cells are in series, stack output is the product of cell potential and number of cells in the stack (N).

$V_{stack} = V_{cell} N$ (27)

## VI. MATLAB SIMULATIONS

### 6.1. Simulation of DC/DC Converter

Simulation analysis of both the converter and the fuel cell model is done using MATLAB/SIMULINK. The proposed and conventional IBCs are realized with the specifications shown next:

1) Input voltage: $V_S$ = 200V.
2) Output voltage: $V_O$ = 24V.
3) Output current: $I_O$ = 10 A.
4) Switching frequency: $f_S$ = 65 kHz.
5) Inductor ripple current: below 3 A.
6) Ripple voltage of a coupling capacitor: below 4V.
7) Output voltage ripple: below 250 mV.

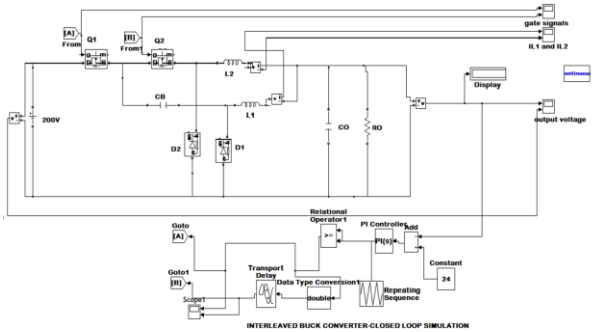


Fig. 7. New IBC with Closed Loop Control.

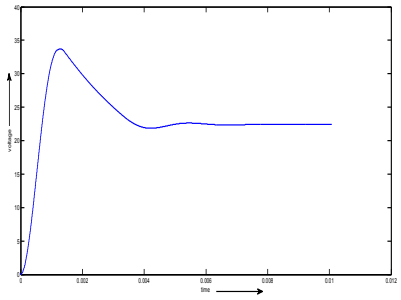

Fig. 8. New IBC Output Voltage

While comparing the simulation results of both conventional and proposed converter, it is found that the voltage conversion ratio has been increased twice in the proposed IBC. Also it is found that the voltage stress across the switches$Q_1$ and $Q_2$ reduced significantly in the case of proposed converter. Voltage stress across $Q_1$ and $Q_2$ in both converters are shown in fig. 12.

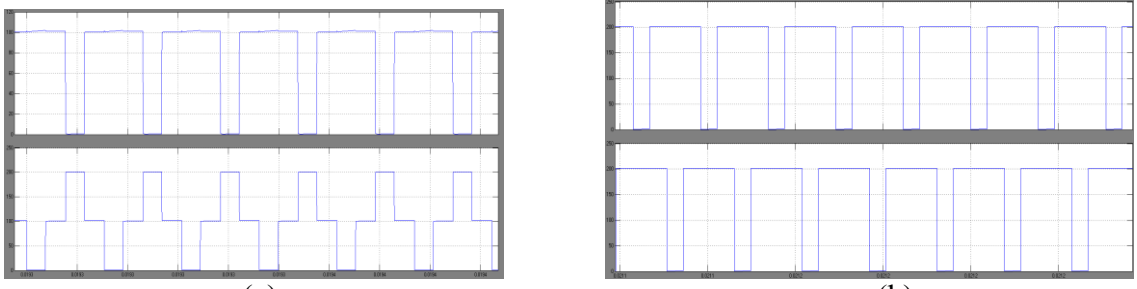

(a) (b)

Fig.9. Voltage stress across (a)Q1 and (b Q2)

### 6.2. Simulation of Fuel Cell Stack

Using the equations (20)-(27) fuel cell can be modeled in MATLAB/SIMULINK. Typical fuel cell has a dc output voltage of about 1.2V. Number of cells can be connected in series to get required output voltage from the stack. Simulink model of fuel cell based IBC is shown in Fig.12.

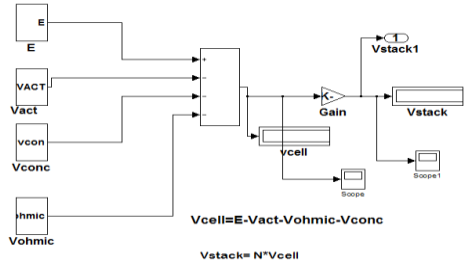


Fig.10. Simulink Model of Fuel cell Stack

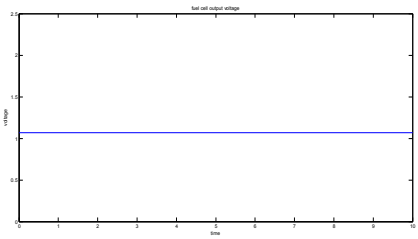

Fig.11. Fuel Cell Output Voltage.

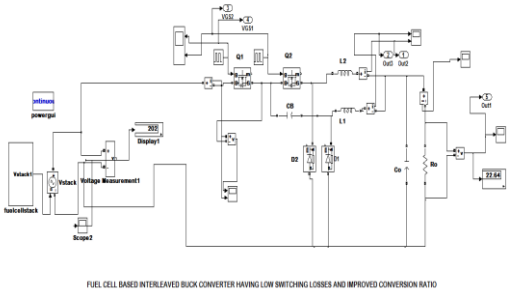


Fig.12. Simulink Model of Fuel Cell Based IBC

## VII. CONCLUSION

The main advantage of the proposed IBC is that since the voltage stress across active switches is half of the input voltage before turn-on or after turn-off when the operating duty is below 50%, the capacitive discharging and switching losses can be reduced considerably. In addition, since the voltage stress of the freewheeling diodes is half of the input voltage in the steady state, the use of lower voltage-rated diodes is allowed. Thus, the losses related to the diodes can be improved by employing schottky diodes that have generally low breakdown voltages, typically below 200V. From these results, the efficiency of the proposed IBC is higher than that of the conventional IBC and the improvement gets larger as the switching frequency increases. Moreover, it is confirmed that the proposed IBC has a higher step-down conversion ratio and a smaller inductor current ripple than the conventional IBC. Closed loop control using PI controller has been done and it is observed that the system performances are improved.

A fuel cell stack is also modelled and simulated. Conventional DC source in the coverter has been replaced by the fuel cell model. Use of such renewable energy sources instead of conventional sources is becoming more popular due to its reliability and availability.

## REFERENCES

[1] Il-Oun Lee*, Student Member, IEEE*, Shin-Young Cho*, Student Member, IEEE*, and Gun-Woo Moon*, Member, IEEE,* "Interleaved Buck Converter Having Low Switching Losses and Improved Step-Down Conversion Ratio," IEEE Trans. on Power Electron., vol. 27, No.8, August 2012.

[2] R. L. Lin, C. C. Hsu, and S. K. Changchien,C. Y. Lin, M. Wu, "Interleaved four-phase buck-based current source with isolated energy-recovery scheme for electrical discharge machine," IEEE Trans. Image Power Electron., vol. 24, no. 7, pp. 2249-2258, Jul. 2009

[3] C. Garcia, P. Zumel, A. D. Castro, and J. A. Cobos, "Automotive DC–DC bidirectional converter made with many interleaved buck stages," IEEE Trans. Power Electron., vol.21, no.21, pp.578-586, May 2006.

[4] C. S.Moo, Y. J. Chen, H. L. Cheng, and Y. C. Hsieh, "Twin-buck converter with zero-voltage-transition," *IEEE Trans. Ind. Electron.*, vol. 58, no. 6, pp. 2366–2371, Jun. 2011.

[5] J. P. Rodrigues, S. A. Mussa, M. L. Heldwein, and A. J. Perin, "Three level ZVS active clamping PWM for the DC–DC buck converter," *IEEE Trans. Power Electron.*, vol. 24, no. 10, pp. 2249–2258, Oct. 2009.

[6] Y. M. Chen, S. Y. Teseng, C. T. Tsai, and T. F. Wu, "Interleaved buck converters with a single-capacitor turn-off snubber," *IEEE Trans. Aerosp. Electronic Syst.*, vol. 40, no. 3, pp. 954–967, Jul. 2004.

[7] Akbari, M. H., "PEM Fuel Cell Systems for Electric Power Generation: An Overview," International Hydrogen Energy Congress and Exhibition IHEC 2005, Istanbul, Turkey, 2005.

[8] Lemes, Z., Vath, A., Hartkopf, Th., Mancher, H.," Dynamic fuel cell models and their application in hardware in the loop simulation," Journal of Power Sources, 154, (2006), 386-393.